# ESF: Report on the visit at Imperial College London

Visitor: Lukas Brinek

Reference Number: 3569

## 0.1 Purpose of the visit

The aim of the visit is the meeting of the collaborators from Prof. T. Šikola (BUT, Czech Republic) and Prof. S. A. Maier (Imperial College London) groups. The present work deals with plasmonic antennas on thin silicon nitride films (thickness 30 nm - 50 nm) in the resonant wavelength range up to 820 nm (the experimental limit). The aim of the project is to detect the electromagnetic field distribution of the plasmonic modes at the antennas by the specially modified transmission electron microscope Titan (FEI-company). HRTEM and EELS (including TEM-BF) measurements are still in progress at Imperial College London and performed by Ai Leen Koh. The work requires checking of many options (e.g.: varying materials, shapes and dimensions of the structures). Not least, the finite-difference time-domain simulations need to be utilized for the confirmation of the experimental results. Lukáš Břínek pursues the FDTD (Lumerical - FDTD Solutions) simulations in that work.

## 0.2 Description of the work carried out during the visit

FDTD simulations (by Lumerical) of the electromagnetic field at the plasmonic structures were concerned during the visit.

## 0.3 Description of the main results obtained

In the simulations of EELS in Lumerical package, excitations localizations in the inner position of the gap between the antenna arms (including the inner vertexes) possess the blue shift in the resonant wavelength compared to the outer vertex localizations of the excitations. This phenomenon was recognized in the real EELS experiments. The simulations and the experiments are in agreement and confirm each other.

## 0.4 Projected publications

The projected articles have not been published.

# 1 Abstract

The present work deals with plasmonic antennas on thin silicon nitride films (thickness 30 nm - 50 nm) in the resonant wavelength range up to 820 nm (the experimental limit). The aim of the project is to detect the electromagnetic field distribution of the plasmonic modes at the antennas by the specially modified transmission electron microscope Titan (FEI-company). HRTEM

and EELS (including TEM-BF) measurements are still in progress at Imperial College London and performed by Ai Leen Koh. Specifically, the finite-difference time-domain simulations in Lumerical package are shown in the report.

# 2 Introduction

Plasmonics deals with the conduction electron oscillations (surface plasmon polaritons) at metal/dielectric interfaces induced by the applied electromagnetic field. The most common source of the electromagnetic field is a plane wave for the surface plasmon polaritons excitations. The recent research reveals a possibility of the plasmon-excitation by localized sources such as the Near Field Scanning Optical Microscopy (SNOM) and the Electron Energy Loss Spectroscopy (EELS). Both the sources are highly localized and have the spatial resolution of about 50 nm for SNOM and 5 nm for EELS. Moreover, the both methods are able to be utilized for spectroscopic measurements. As the plasmonic structures operating at optical wavelengths have dimensions of about tens to hundreds nanometers, EELS is the appropriate method for detections of the distribution of the near field.

The aim of the project was to determine the difference between the localized excitation of surface plasmon polaritons at the antenna by EELS and the excitation by plane waves. Subsequently, the coupling between the antennas in the group and the resulting shift of resonant wavelengths are studied. Resonant spectra and also distributions of the near field are concerned. In this work, the equilateral-triangular-arms antennas of the side size 110 nm are simulated. Size scales in the pictures miss the numeric values as the size of every one plotted arm is of the same dimension.

# 3 One-arm antenna

## 3.1 Excitation by plane waves

Spectra acquired from simulations of the plane wave scattering by one-arm antenna are shown in Fig. 1 for two perpendicular polarizations. There are two modes for the both polarizations. For the scattering, the first mode occurs at $\lambda = 833\,\mathrm{nm}$; the second mode occurs at $\lambda \doteq 600\,\mathrm{nm}$. For the near field, the first mode occurs at $\lambda = 840\,\mathrm{nm}$; the second mode occurs at $\lambda \doteq 560\,\mathrm{nm}$.

The x-components $P_\mathrm{x}$ of the Poynting vector at the top of the antenna are depicted in Fig. 2 for the both modes in TM polarization [1]. For the both modes of the TE polarization, the y-components $P_\mathrm{y}$ of the Poynting vector at the top of the arm are depicted in Fig. 3 [2]. For the both polarizations, the first mode is the dipole mode and the second mode seems to be the quadrupole mode. The electric intensities for the resonant wavelengths are enhanced in respect to the polarizations of the incident field and the mode order (see Fig. 4).

## 3.2 "EELS" excitation

In Lumerical, EELS is simulated by a line (a row) of dipoles excited with the defined delays corresponding to the velocity of the moving electron in the real EELS experiments. Such a model hardly describes the problem completely, however, it provides the proper description. EELS signal in Lumerical is given by the $P_z$ component of the Poynting vector at the horizontal

[1] The further components of the Poynting vector are small.
[2] The further components of the Poynting vector are small.

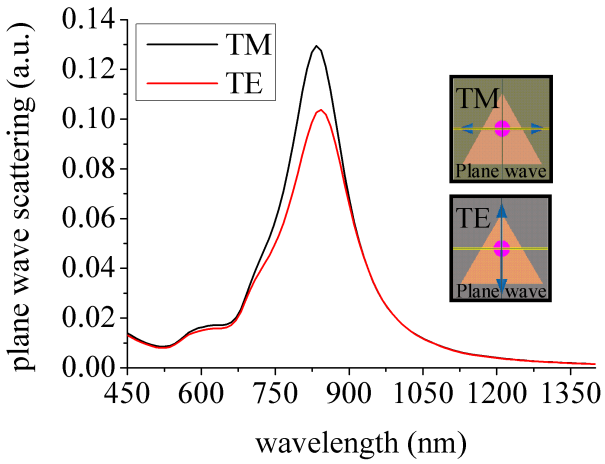


Figure 1: Spectra of one triangular arm antenna excited by plane waves with perpendicular polarizations.

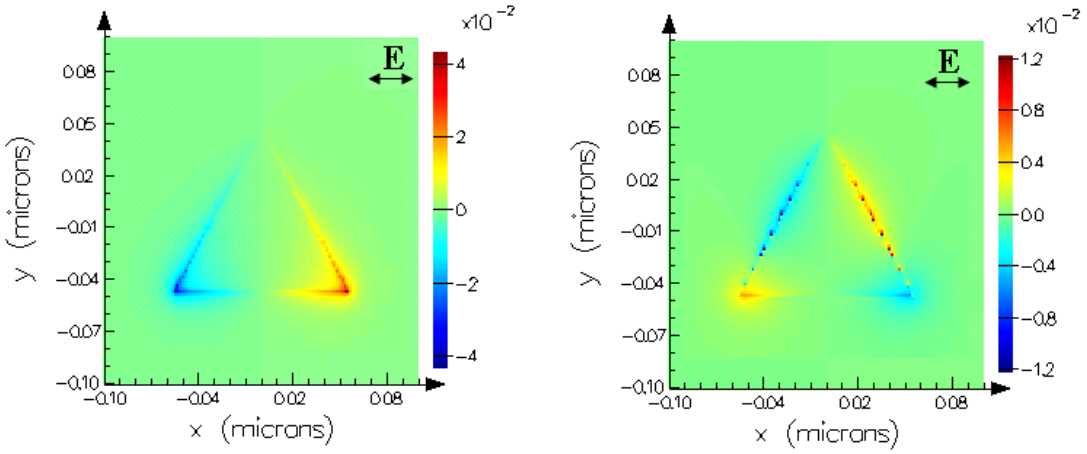


Figure 2: The x-components $P_x$ of the Poynting vector for the both modes (at $\lambda = 863$ nm and $\lambda \doteq 600$ nm respectively) for TM polarization.

monitor around the antenna.

Spectra of EELS simulated in Lumerical differ by the excitation localization at the antenna. The difference between the spectra is obvious from Fig. 5. Only one peak (mode) appears in the spectra taken for the excitation in the vertex-excitation point (see inset in Fig. 5). The resonant wavelength for the vertex excitation point is about 853 nm.

Consequently, two modes (peaks) can be excited for the excitation point at the side of the arm (see inset in Fig. 5). The first mode is excited at the wavelength of about 853 nm, which is the same as for the vertex excitation. However, the second mode occurs at the resonant wavelength of about 581 nm. Fig. 5 also depicts the simulated EELS spectra for the different velocities of the moving electron.

In the resonant wavelength position, there is the difference between the far field scattering and the near field in the plane waves excitation. The resonant wavelength in EELS corresponds more to the near field resonant wavelength, because the moving electron is sensitive to the near field at the antenna which is higher than the far field. Such differences were observed also

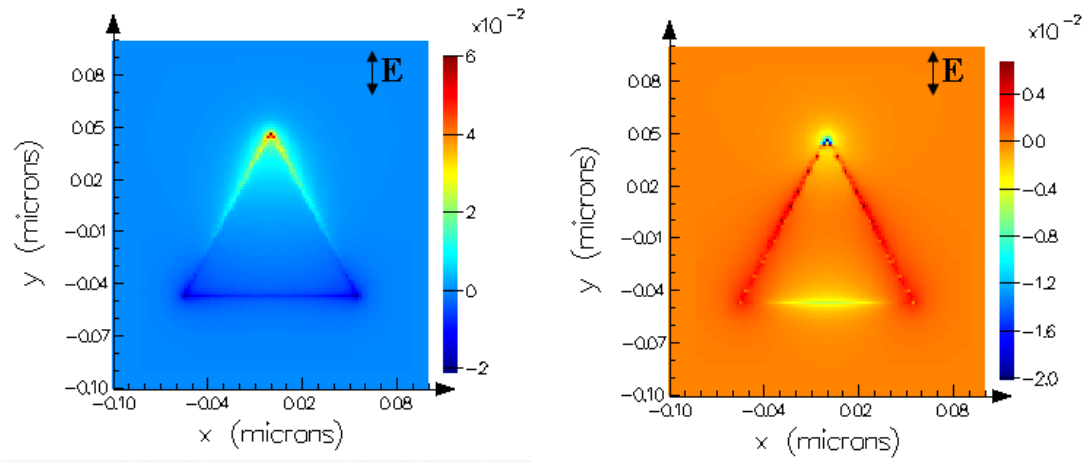


Figure 3: The y-components $P_y$ of the Poynting vector for the both modes (at $\lambda = 863$ nm and $\lambda \doteq 600\,\mathrm{nm}$ respectively) for TE polarization.

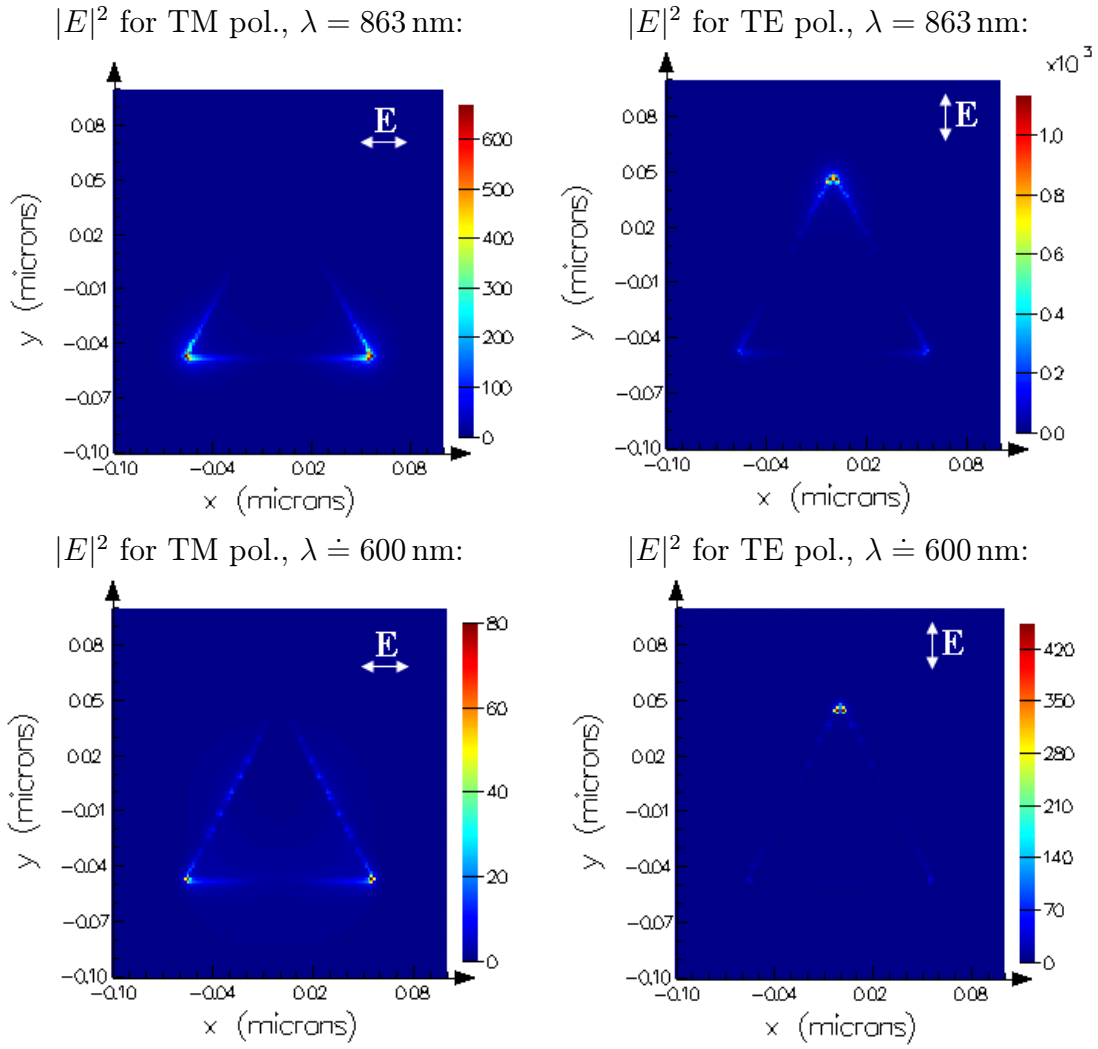


Figure 4: The electric intensities $|E|^2$ for the both modes (at $\lambda = 863\,\mathrm{nm}$ and $\lambda \doteq 600\,\mathrm{nm}$ respectively) for TM and TE polarizations of the incident field.

experimentally.

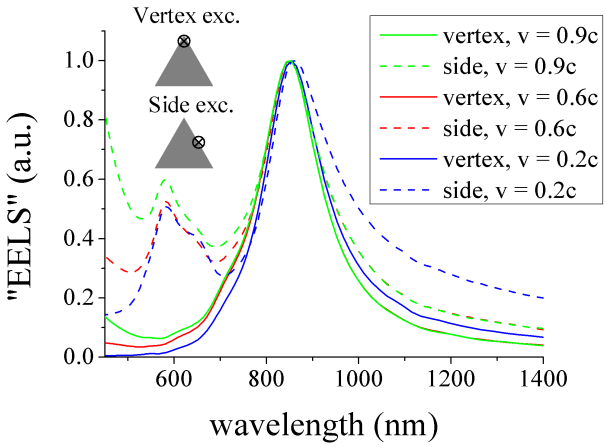


Figure 5: EELS spectra for the excitations in the different excitation points, i.e.: in the vertex and at the side of the arm. The depicted spectra are taken from simulations concerning different velocities of the moving electron (i.e.: $v = 0.2c$, $v = 0.6c$, $v = 0.9c$).

The $P_z$ fields at the top of the antenna for the resonant wavelengths are shown in Fig. 6 for the vertex and side excitations.

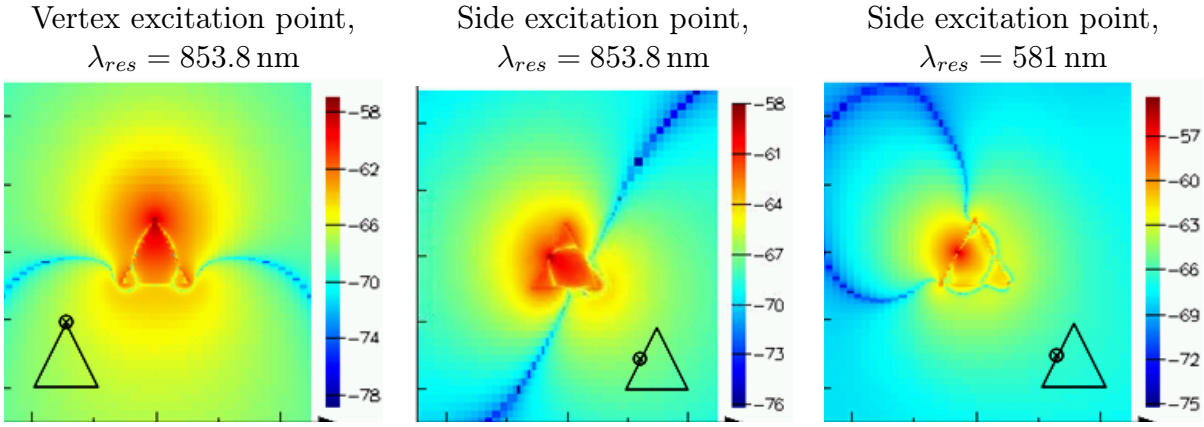


Figure 6: Simulated EELS. The log(real($P_z$)) fields for the resonances at the top of the antenna for the vertex and side excitations.

# 4 Two-arms antenna

Spectra of the plane wave scattering by two-arms antenna are compared to the scattering spectra by one-arm antenna. For TM mode, the resonant wavelength of two-arms antenna shows the slight blue shift of about 5 nm compared to the one-arm antenna resonant wavelength. For TE mode, there is the red shift of about 115 nm of the resonant wavelength for the two-arms antenna compared to the one-arm antenna (see Fig. 7). The subsequent pictures in Fig. 8 depict the appropriate components of the Poynting vector for the resonances [3].

For EELS simulated in Lumerical, the graph in Fig. 9 expresses the blue shifted resonant wavelength for the two-arms antenna excited in the point in the middle of the gap compared

[3]The further components of the Poynting vector are small.

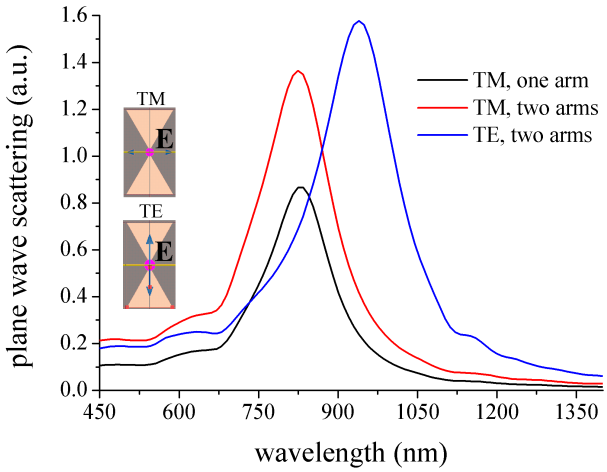


Figure 7: Spectra of plane wave scattering by one- and two- arms antennas for TM and TE polarizations.

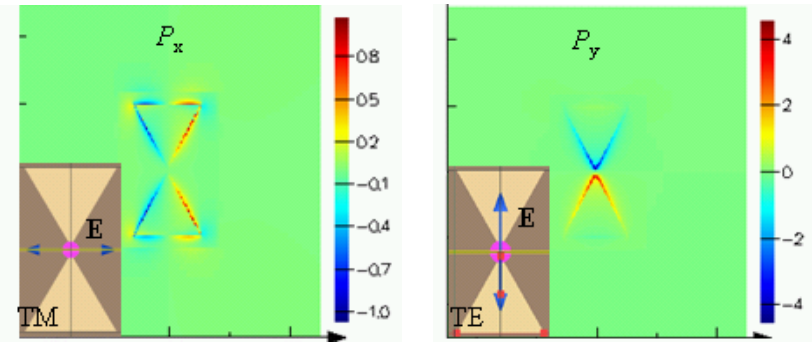


Figure 8: Plane wave scattering. Components of the Poynting vector for TM and TE polarizations at two-arms antenna at the resonances.

to the one-arm antenna. In particular, $P_z$ components of the Poynting vector for one-arm and two-arms antennas excited by EELS in the middle of the gap are shown in Fig. 10. The field distributions seem to be similar.

The gap dependence of the two-arms antenna excited by EELS in the middle of the gap is shown in Fig. 11.

# 5 Three-arms antenna

The plane wave scattering spectra for the three-arms antenna for two perpendicular polarizations are shown in Fig. 12. The fields for the corresponding resonant wavelengths are depicted in Fig. 13. The field at the resonant wavelength of about 900 nm represents the dipole mode; the resonant wavelength of about 600 nm seems to be the quadrupole resonance.

EELS spectra for the different inner vertex excitation points, for the excitation in the middle of the gap, and for the outer vertex excitation points are depicted in Fig. 14. The spectrum b) II. is almost the same as the resonant spectrum of one-arm antenna excited by EELS at the vertex. It represents the un-coupling state which is also obvious from the picture b) II. in Fig. 16 and Fig. 6.

The extensive overview of the spectra taken from simulations with various excitation points is plotted in Fig. 15. The inner vertex point possesses the broad peak from 750 nm to 891 nm.

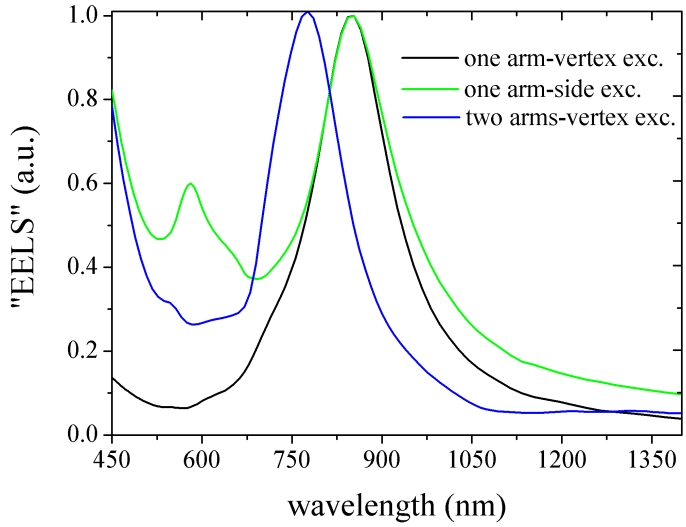


Figure 9: Simulated EELS. Comparison of the spectra of one- and two-arms antennas excited in the point in the middle of the gap.

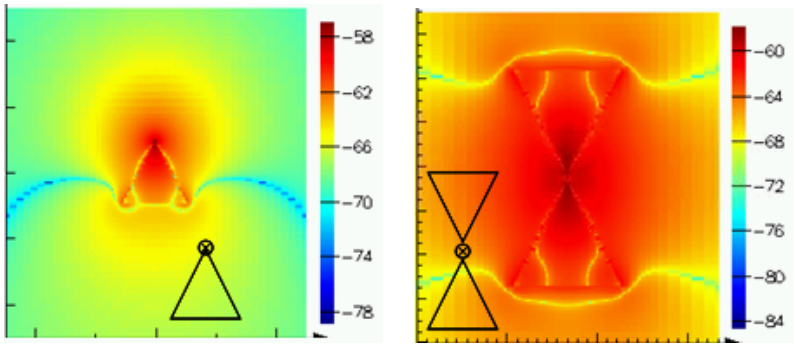


Figure 10: EELS pictures of log(real($P_z$)) for one-arm and two-arms antennas excited in the middle of the gap.

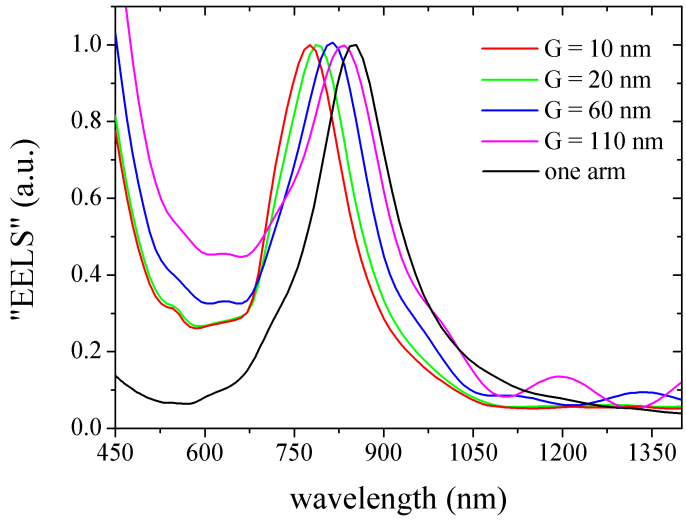


Figure 11: Simulated EELS. The gap dependence of the two-arms antenna excited in the middle of the gap.

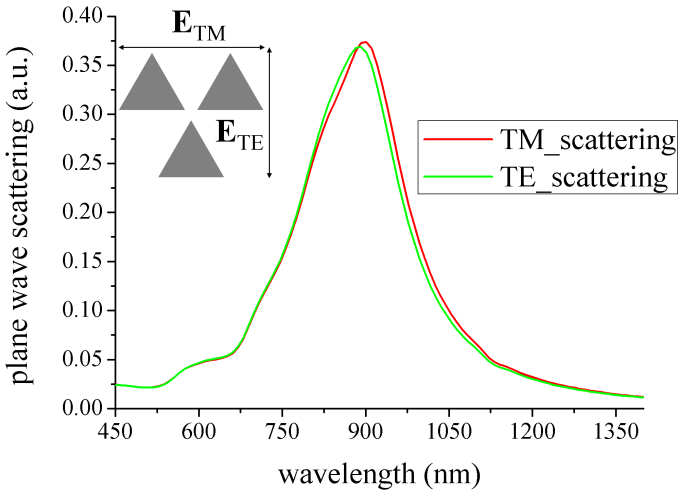


Figure 12: The plane wave scattering spectra of the three-arms antenna with the perpendicular polarizations.

Only 5 nm spacing of the excitation point at the inner vertex to the middle of the gap results the grow of the peak at 750 nm.

The excitation points in the inner positions of the gap possess the blue shift in resonant wavelength compared to the outside vertex excitation points. The excitations in the excitation points in the outer vertexes result in the almost un-coupling states; the excitations in the excitation points in the inner vertexes result in the coupling states with the blue shifted resonances. This phenomenon was recognized in the real EELS experiments. The simulations in Lumerical confirm the experiments by the way. The corresponding pictures of log(real($P_z$)) field at the resonant wavelengths are plotted in Fig. 16 for the different excitation points.

# 6 Conclusion

The excitation localizations in the inner position of the gap possess the blue shift in resonant wavelength compared to the outside vertex points resonances. The only 5 nm shift at the inner vertex point to the middle of the gap possesses also the blue shift. This phenomenon was recognized in the real EELS experiments. The simulations and the experiments are in the agreement.

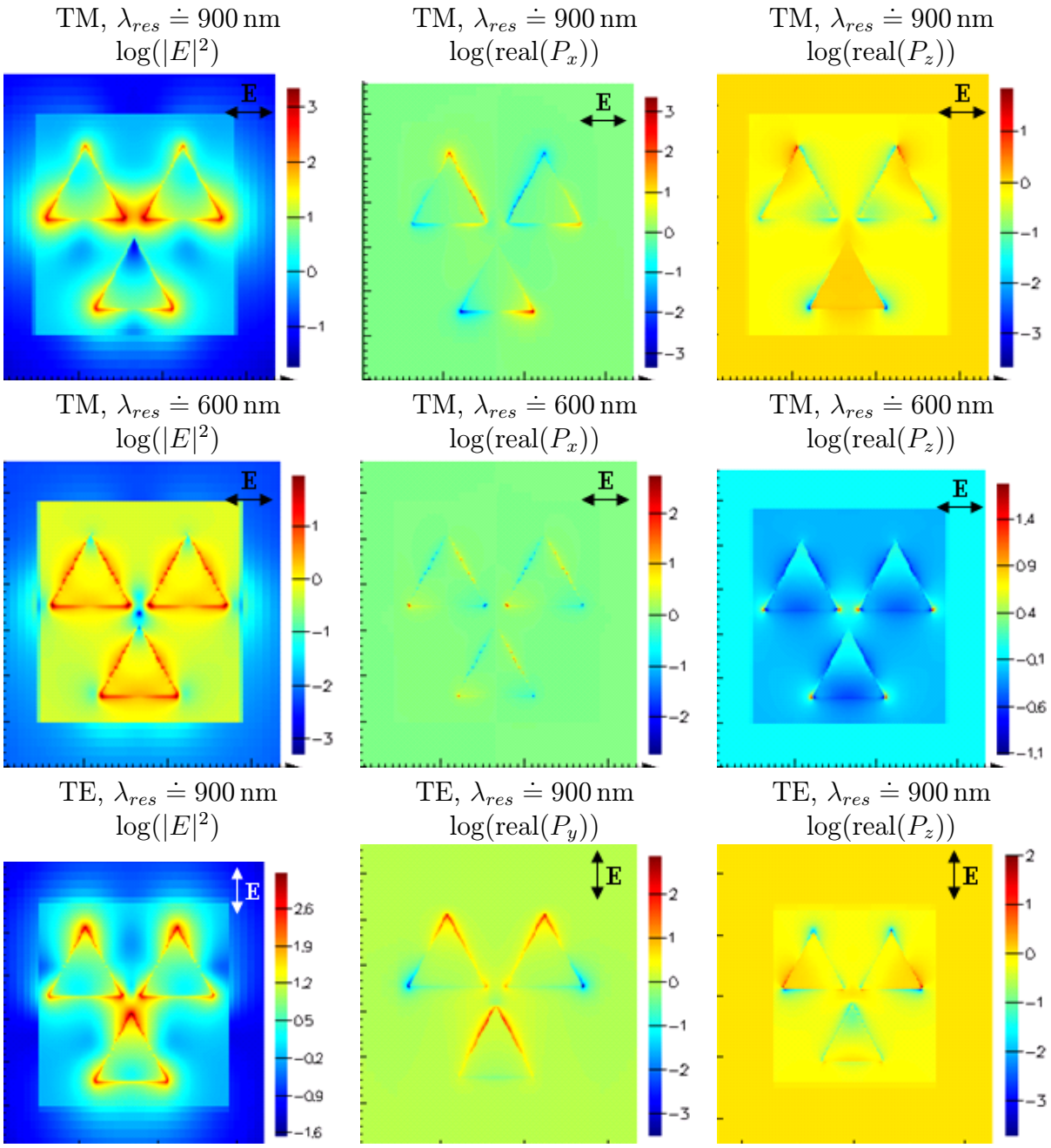


Figure 13: The field pictures for the plane wave scattering by three arms antenna for TM and TE polarizations.

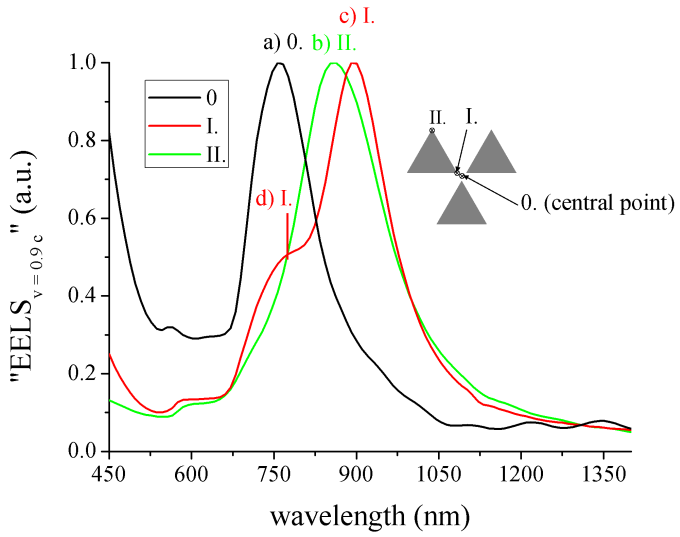


Figure 14: EELS spectra for the different excitation points at the three-arms antenna. The excitation points are plotted in the inset.

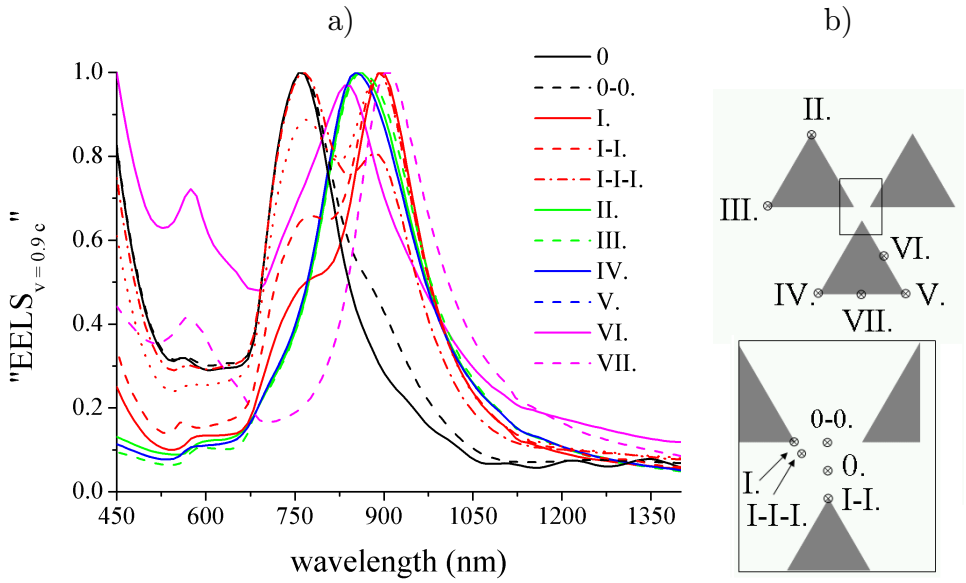


Figure 15: A) Spectra taken from simulations of EELS for different excitations points. Points 0. and 0-0. are the excitations point in the middle of the gap; I., I-I., I-I-I. are the inner vertex excitations points; II., III., IV., V. are the outside vertex excitations points; VI. and VII. are the side excitations points. B) The map of positions of the excitations points.

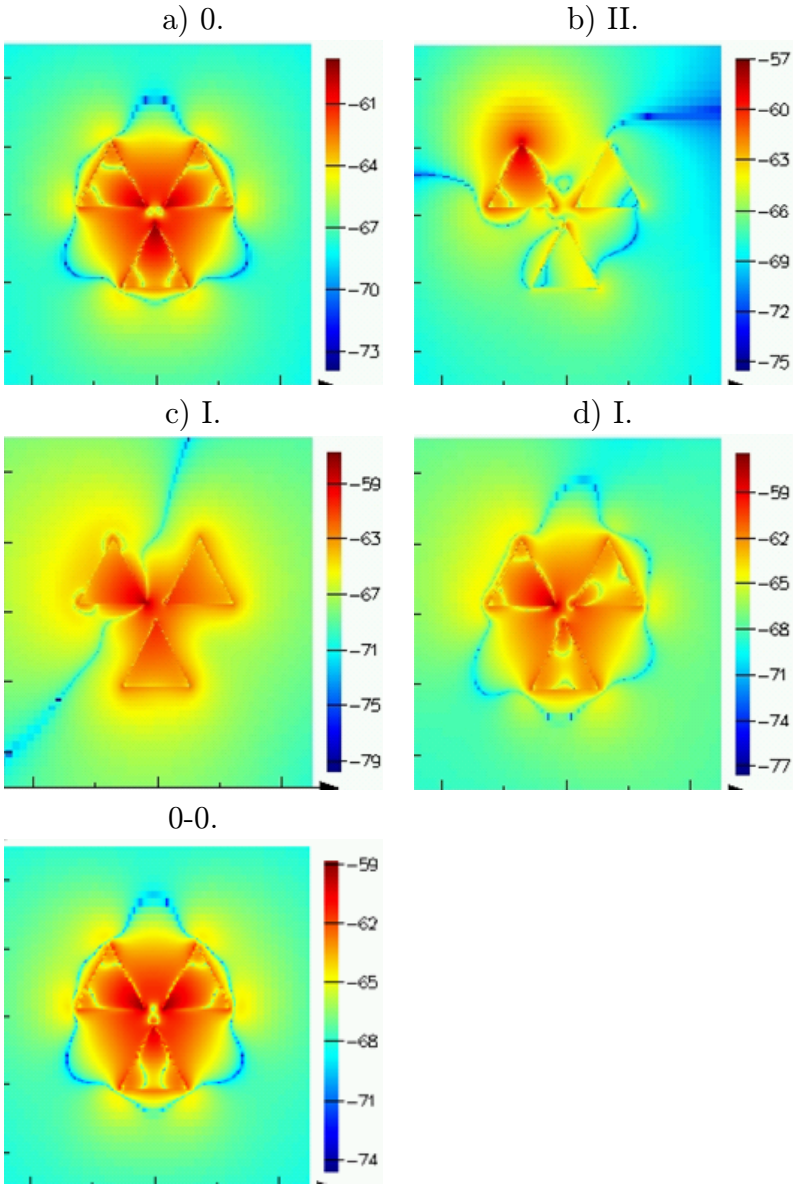


Figure 16: Pictures of log(real($P_z$)) field in the simulated EELS at the resonant wavelengths for different excitation points at the top of the antenna.